Specific binding of aminoglycoside antibiotics to RNA

Yong Wang and Robert R Rando*

Department of Biological Chemistry and Molecular Pharmacology, Harvard Medical School, 250 Longwood Avenue, Boston, MA 02115, USA

Background: Aminoglycoside antibiotics interfere with ribosomal protein synthesis and with intron splicing. Various lines of evidence suggest that RNA is the molecular target for aminoglycosides, but little is known about the recognition process. Is recognition of a particular aminoglycoside specific for certain RNA structures? If so, what are the rules for recognition? We have begun to investigate this problem by *in vitro* selection of RNA molecules that can specifically bind to the aminoglycoside antibiotic tobramycin.

Results: An RNA diversity library was used to select for sequences capable of binding to the aminoglycoside antibiotic tobramycin. After six cycles of selection, 82 % of the RNA bound to tobramycin specifically. The selected RNA was reverse-transcribed into DNA, which was then cloned. At low selection stringency, an extremely large number of clones, on the order of 10^7, produced RNAs capable of binding tobramycin with K_ds in the μM range (values similar to that observed for the binding of tobramycin to *Escherichia coli* ribosomes). Sequencing of 18 of the clones revealed no obvious consensus sequence. At higher selection stringencies (K_ds in the nM range) only two consensus sequences for binding were observed.

Conclusions: We have shown that RNA molecules can be readily selected that bind the aminoglycoside tobramycin. The RNAs that bind tobramycin with high affinity contain consensus binding regions that may be confined to predicted stem–loop structures. These studies open the way for understanding the basis of RNA–aminoglycoside recognition.

Chemistry & Biology May 1995, **2**:281–290

Key words: aminoglycosides, fluorescence, *in vitro* selection, RNA

Introduction

Antibiotics that interfere with protein synthesis often bind to ribosomal RNA (rRNA) rather than to ribosomal proteins. Substantial evidence in support of this view has been reported. Resistance to various antibiotics often involves methylation at specific sites in rRNA [1]. The antibiotic thiostreptone binds tightly to a 60-nucleotide sequence (60-mer) from rRNA [2]. Aminoglycosides and peptide antibiotics can inhibit group I intron splicing by binding to specific regions of the RNA [3,4]. Certain aminoglycosides and other protein-synthesis inhibitors have also been found to interact with specific bases in 16S rRNA [5]. Interestingly, a molecular basis for hypersensitivity to aminoglycosides has been localized to a single base change in mitochondrial rRNA [6]. Along these lines, an oligonucleotide analog of the 16S rRNA has also been shown to interact with certain aminoglycosides [7]. It has been suggested that there may be common features in the modes of recognition of aminoglycoside antibiotics with self-splicing introns and with the decoding regions of 16S rRNA [8]. Recent studies have also shown that aminoglycosides can bind to a hammerhead ribozyme [9] and can also block the binding of the HIV Rev protein to its viral RNA recognition element [10]. While these kinds of experiments implicate RNA as the target for various antibiotics, including the aminoglycosides, there are no reports demonstrating the specific binding of any aminoglycoside to a particular domain of an RNA molecule.

From the observations described above it is probable that rRNA is a target for many of the antibiotics that inhibit protein synthesis. This notion is consistent with the chemical properties of the antibiotics and rRNA. For example, the aminoglycosides, which are a particularly well studied and important group of antibiotics, are polycationic saccharides at neutral pHs and would be expected to interact effectively with RNA both through electrostatic interactions and through hydrogen bonding. It would be of substantial interest to determine what kinds of RNA structures are recognized by molecules like the aminoglycosides. Are the numbers of such structures limited, and if so what are they?

To address these issues, we have begun to explore the use of *in vitro* selection of aptamers from RNA diversity libraries [11–13] to define the kinds of RNA molecules that bind to a particular aminoglycoside, in this case tobramycin. Figure 1 shows the structures of tobramycin and its analogs, 6'-N-acetyl tobramycin and 6'-N-4-pyrenebutyryl tobramycin. Tobramycin has practical advantages for these kinds of studies, because it can be specifically acetylated at the less hindered 6' primary amino group to provide useful analogs for molecular studies [14,15]. Moreover, the acetylated tobramycin analogs that have been tested retain biological activity [15]. In this article we show that an assortment of RNA molecules that can be selected from a random RNA pool can specifically recognize tobramycin. Selections were performed using a tobramycin affinity column at

*Corresponding author.

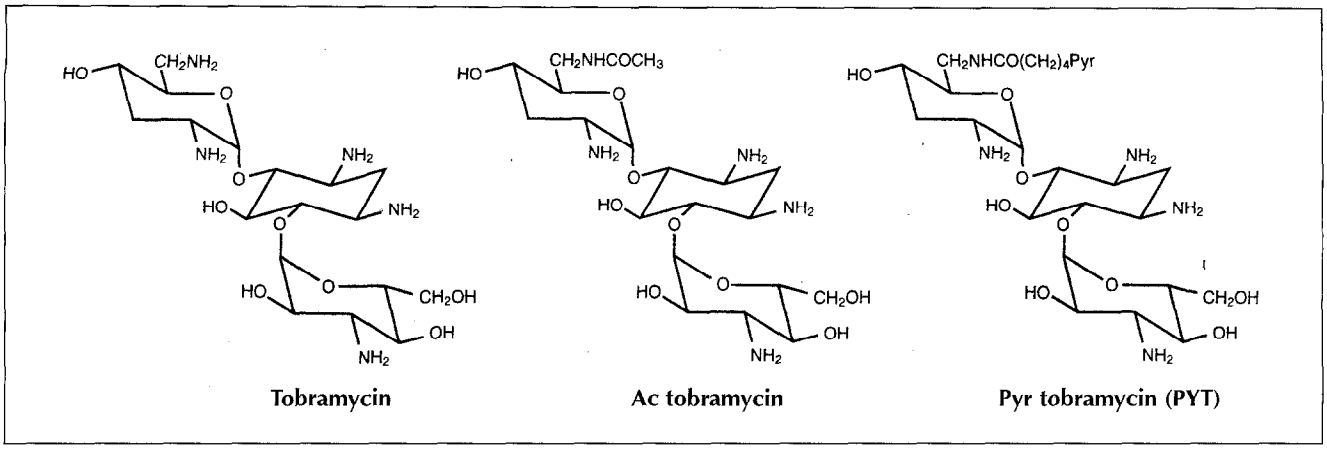

Fig. 1. Structures of tobramycin and analogs used in these studies.

different densities of the coupled drug. Binding was analyzed with PYT (Fig. 1), a pyrene-butyramide-labeled fluorescent derivative of tobramycin.

Selections were initially performed at low stringency. The K_d for tobramycin binding is 4.3 μM, and that for PYT is 200-fold less (20 nM) for one particular RNA molecule selected at this stringency with one tobramycin binding site per molecule. By using the fluorescence assay it was also determined that, overall, the pool of RNAs selected at low stringency binds PYT with a K_d of 52 ± 8 nM, and tobramycin with a K_d of 8.8 ± 0.3 μM. When selections were performed at higher stringencies, tighter binding RNAs were found, containing one of two consensus sequences. These consensus sequences were confined to predicted stem–loop structures, as demonstrated by independent synthesis. The binding of tobramycin to these aptamers proved to be in the nM range. These data show that tight-binding RNA molecules can readily be selected for aminoglycoside antibiotics. Moreover, as the stringency of selection is increased the number of RNA molecules capable of binding to aminoglycosides radically decreases. Structural studies on the selected RNA molecules should shed light on the rules that govern specific aminoglycoside–RNA binding interactions.

Results

Selection of RNA molecules that bind to immobilized tobramycin

Initial studies were focused on the interaction of the random RNA pool with the tobramycin affinity column described below (see Materials and methods). This column was prepared using 20 μmoles of tobramycin to couple to 15 μmoles of N-hydroxysuccinimide-reactive sites per ml on the column. This 'low stringency' column was used in the initial selections to obtain as many sequences as possible that could recognize tobramycin. The randomized pool consisted of 109-mer RNA transcripts containing 60 central randomized bases flanked by PCR primer sequences containing a T7 RNA polymerase promoter. This pool of RNAs was transcribed from a pool of aptamer DNA plasmid constructs, designed as previously described [16]. The original ^{32}P-labeled RNA pool was produced by transcription of 120 μg of the DNA pool. Elution patterns of the RNA from the columns are shown in Figure 2 for the second and sixth selections. Over six cycles of selection, the percentages of RNA specifically eluted with 10mM tobramycin were <0.1 %, 3.0 %, 2.9 %, 26 %, 55 % and 82 %. Further selections did not increase the specific binding pool. The RNA pool transcribed from DNA after the sixth selection could not be eluted from the affinity column, even after 100 column volumes of selection buffer were passed through the column. Furthermore, 10 column volumes of selection buffer containing 50 mM D-glucosamine did not cause any bound RNA to be eluted from the column, while 96 % of the RNA could be eluted with three column volumes of 10 mM tobramycin. The observation that D-glucosamine did not cause the elution of the bound RNA suggests that the binding interaction is specific.

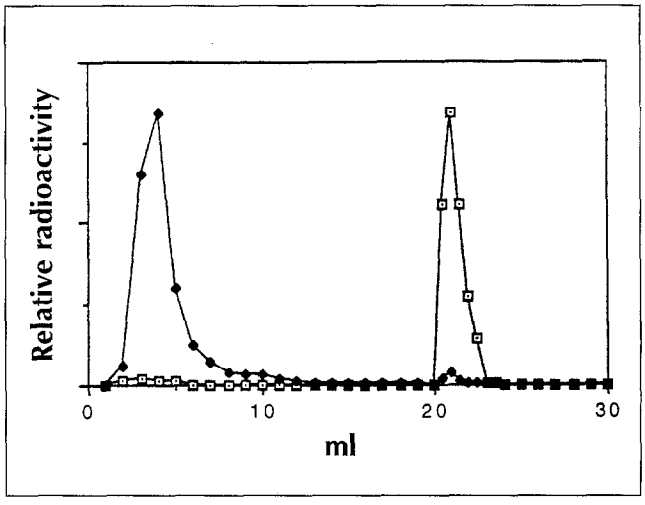

Fig. 2. The elution profiles for cycle 2 (◆) and cycle 6 (□) of the low-affinity aptamer selection. After the tobramycin affinity column was washed with 20 column volumes of selection buffer, bound RNA was specifically eluted with 10 mM tobramycin in selection buffer.

```
 1. 5'...AAUUGGAUCAUACUGUUAUAAGUAGGUGGCUCAGCGGUUGCCUUCGGCAGGUUGAUCCGU...3'
 2. 5'...GUGGUAUAUCCUGGUUGUGCGUAUGUACUCCGGCUUCUAUAGUUCUGGUUGGUGGCGGAC...3'
 3. 5'...UGUGAUAGGACUGUGAUUCGGAUCAUGUUGUGAACAUGGUGUGCAUCAUGGGGAGCCCGU...3'
 4. 5'...CUCAUUCACGGGAUGGCUCUUACACAGUCUGUGUAGGGCGUCGCGUGUGGUUAUGUUGGC...3'
 5. 5'...UUCACGGCAUAAUUCUGUUUGAGUUGGCCUUUUGGUAAUGUAGCGUGGGUUUGCGGUGCG...3'
 6. 5'...CCUGUGGGGCGUACGUUGGUACAAGAGGUUAGGUGGCCUAAUGUAGCCUACGUGCGGCGU...3'
 7. 5'...CUGCUGCAGUUGUUAUGGGCCGUUCUAACUGGGGUGGUACCCGACCGAGUCAGCAGGUG....3'
 8. 5'...CGUUUGGGGUCCCACAACACAGGUCUUUGCUGGUCAUAUAUGCGUGUCCUCUAGGAAGUG...3'
 9. 5'...CGUAAAUGGCGCAACGUCGCUCAUGUCGGGUUGGCCAAGUUUCAUUUGCGUUGUCUCAGU...3'
10. 5'...GGCGUUCAGCGGUUCUUCGGGUAAGGCCGUGAGUGUGCGUACGUGAGGGUUAACGCCGU....3'
11. 5'...UAUGUUGCACCCACUGCGGUUCAGUUAUGGUUGUUUCGGCCAUUUGGUUCGCAGCUGUGA...3'
12. 5'...GGUCAGGCGUCUCAUGUAGUUUGUUCCUGUGUAUAUUUGCUCUCUUCGGGGACACCCUGUC..3'
13. 5'...AGUGAUUAUCACAACAGUAUGUCUGGUUGCUCAUGGAGGUUGCAUUGAGGCUAUUAGUAG...3'
14. 5'...UCAAGUCCUGUCUGGUGCGCCUACAGGAUUGGGAUCAUGGGUGUCAAGCAUUUGUGUC.....3'
15. 5'...CACGGUAAAGUAGCAUUGUUCGUUUCCUUGUUUUACUACUCGUAGUGACAGCAGAUGCUG...3'
16. 5'...UGUGUUGCUACGAGGUUGGCCAAUAUGUAGCGUUGCUGCAUAGUGGUUGUCUUAUAUCUG...3'
17. 5'...UGCAGGCUUUUGGCUGUGGGUUUAUGUCCAUGUGUUAGAUCAGCGUUUUACGGUUAGCGC...3'
18. 5'...CCACUAGGCUACAUAGGCGUACAUCCUUCCCGGAGGUCUUAGCGCCGCUAUGGGGUUGGA...3'
```

Fig. 3. Nucleotide sequences of low-affinity aptamers. The sequence of the random region of 18 clones is shown. Total sequence: 5'-GGGAGAAUUCCGACCAGAAGCUU-random region-CAUAUGUGCGUCUACAUGGAUCCUCA-3'.

Cloning and sequencing of the selected pool

RNAs eluted after the sixth round of selection were reverse-transcribed and cloned. We sequenced 18 of the clones to determine if there were consensus sequences. As can be seen in Figure 3, no obvious consensus sequence was observed.

We investigated 10 RNA aptamers (clones 1–10) prepared from these clones and showed that they bound specifically to the affinity column, as they could not be eluted with more than 100 column volumes of selection buffer, but were eluted with 3 column volumes of selection buffer containing 10 mM tobramycin.

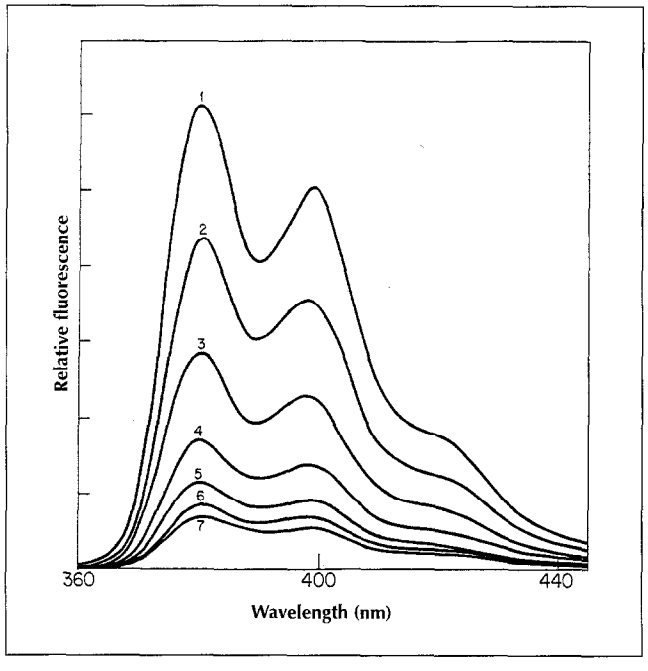

Fig. 4. Fluorescence emission spectra of PYT solution in the presence of varying concentrations of W13 RNA. [PYT] = 151 nM. [W13-RNA]: **1**, 0; **2**, 0.056 μM; **3**, 0.112 μM; **4**, 0.224 μM; **5**, 0.44 μM; **6**, 0.7 μM; **7**, 1.1 μM.

Dissociation constant measurements on an aptamer

One of the clones (shown as clone 8 in Fig. 3; henceforth referred to as W13) was chosen for quantitative studies to determine the specificity of its binding to tobramycin. Using equilibrium dialysis, the K_d for ^{3}H-acetyl tobramycin (Fig. 1) was determined to be 1.3 μM. The K_d for tobramycin was determined to be 3 μM by competition studies with ^{3}H-acetyl tobramycin. These values are close to those measured for tobramycin and ^{3}H-acetyl tobramycin binding to ribosomal targets [15].

Equilibrium dialysis measurements are not well suited for detailed studies on tobramycin binding, because of practical limitations in the available specific activity of the ^{3}H-acetyl tobramycin. To study the binding behavior of W13 carefully, the fluorescently labeled pyrene conjugated tobramycin derivative PYT was prepared (Fig. 1). Pyrene derivatives are useful for studying RNA interactions, as the fluorescence intensity can be markedly affected by binding to RNA [17,18]. In the present case, the fluorescence emission intensity of PYT proved to be strongly quenched upon addition of W13 RNA (Fig. 4), indicating complex formation between the RNA and the ligand. The very large dynamic range (>10) observed here makes careful quantitative studies on binding possible. The fluorescence intensity of PYT as a function of RNA concentration fits an equation for a 1:1 complex (see Materials and methods) very well, as shown in Figure 5, giving a $K_d = 20 \pm 4$ nM. This means that there is a tight 1:1 complex formed between the antibiotic and RNA. Competition experiments show that tobramycin competes with PYT for binding to the RNA (Fig. 6). Curve fitting using the fluorescence intensity of PYT as a function of the tobramycin concentration gave a $K_d = 4.3 \pm 0.7$ μM for tobramycin (Fig. 7). Therefore PYT binds to W13 > 200 times more tightly than does tobramycin itself. Other antibiotics and glucosamine were also tested for their abilities to bind specifically to W13 RNA. As can be seen in Table 1, glucosamine does not bind, and erythromycin binds

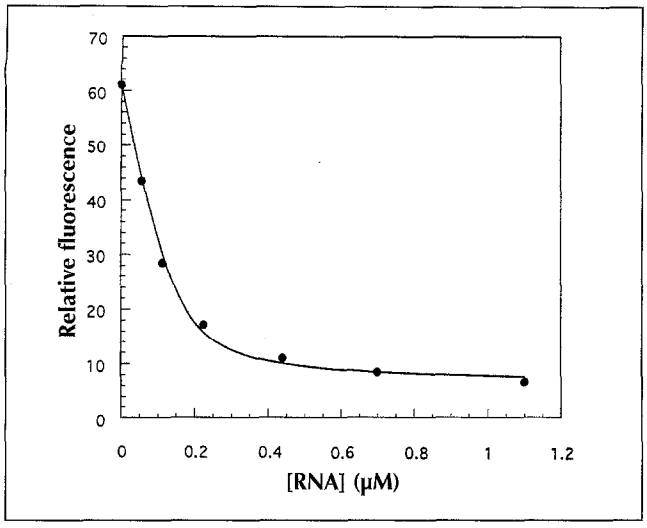

Fig. 5. Fluorescence titration of PYT as a function of W13 RNA concentration. The solid line is calculated using Equation 1 described in Materials and methods (curve obtained by curve fitting).

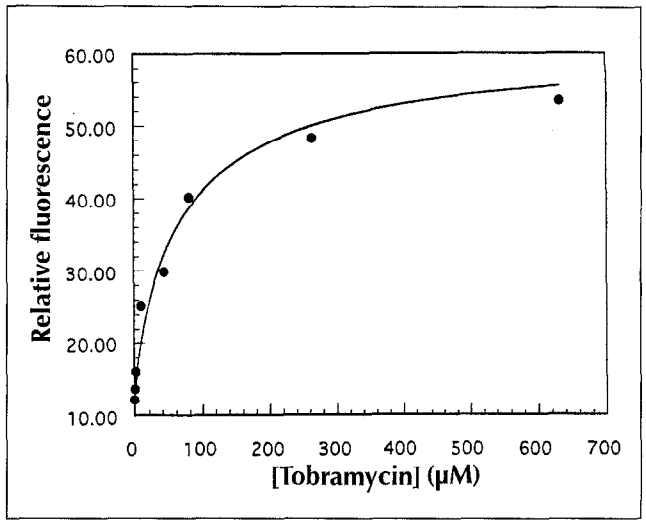

Fig. 7. Fluorescence titration of PYT solution containing W13 RNA as a function of tobramycin concentration. The solid line is calculated using Equation 2 described in Materials and methods (curve obtained by curve fitting).

relatively weakly. On the other hand, the aminoglycoside antibiotics gentamycin and in particular neomycin, both of which are structurally related to tobramycin, bind well to W13 RNA.

The results described above demonstrate that one of the selected clones can bind to tobramycin with a relatively high affinity. It is possible that we were just fortunate in choosing this clone. To address this issue, the average K_d values for the selected random pool was measured. Using the fluorescence assay we found that, overall, the selected pool mixture binds PYT with a K_d of 52 ± 8 nM, and tobramycin with a K_d of 8.8 ± 0.3 μM (data not shown). Therefore, the clone chosen for analysis (W13) is representative of the average binding capacity of the selected random pool.

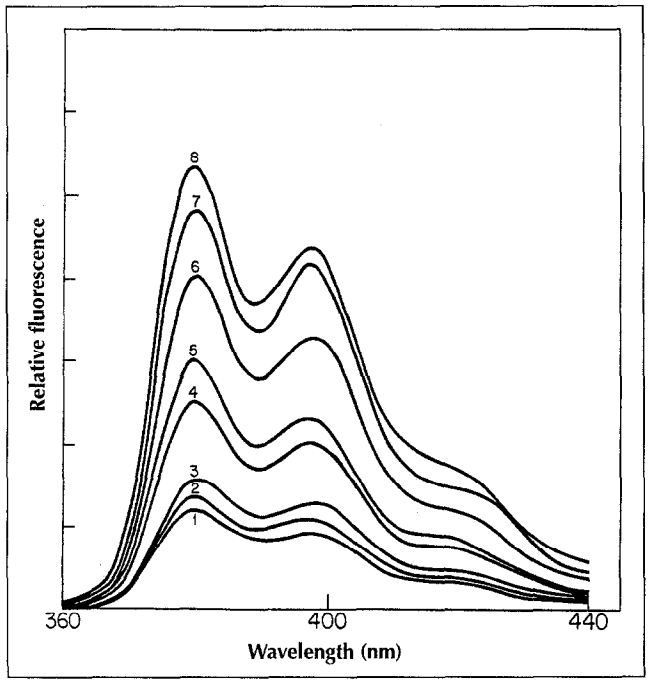

Fig. 6. Fluorescence emission spectra of PYT solution containing W13 RNA in the presence of varying concentrations of tobramycin. [PYT] = 152 nM. [W13 RNA] = 300 nM. [Tobramycin]: **1**, 0; **2**, 0.73 μM; **3**, 2.57 μM; **4**, 10.06 μM; **5**, 44.86 μM; **6**, 81.39 μM; **7**, 264.85 μM; **8**, 631.76 μM.

Reselection for higher affinity aptamers

While the average K_d for the previously selected RNA pool is in the μM range, it is likely that there are also higher affinity aptamers in this mix that are infrequently represented in the pool. The fact that no consensus sequence was observed in the previous selections shows that the selected pool is not close to exhaustion with respect to tobramycin-binding aptamers. A new Affi-Gel was prepared using 0.075 μmoles tobramycin per ml of gel in the coupling reaction instead of 20 μmoles tobramycin per ml of gel. The RNA pool that was obtained after the sixth cycle of the first selection was reselected against this new gel. Over seven cycles of selection, the percentages of RNA specifically eluted with 10 mM tobramycin were 0.3 %, 4.9 %, 6.6 %, 21.9 %, 9.1 %, 50.7 % and 86.1 %, for a total amplification of ~1.2 x 10^7. When RNAs from this selected pool were cloned and ~40 of the clones were

Table 1. Dissociation constants of W13 RNA to antibiotics.

	K_d (μM)
PYT	0.020±0.007
Tobramycin	4.3±0.7
D-Glucosamine	N.B.*
Erythromycin	505±25
Gentamycin C	47±11
Neomycin B	4.7±0.9

Binding was determined at 20 °C. D-Glucosamine was used as a control for non-specific binding. *N.B., no detectable binding.

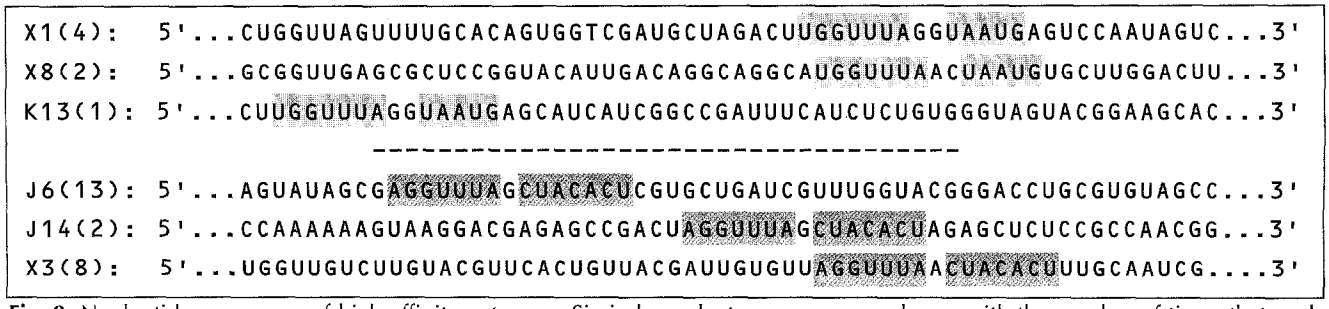

Fig. 8. Nucleotide sequences of high-affinity aptamers. Six independent sequences are shown with the number of times that each sequence was obtained indicated in parentheses. The sequences fall into two groups. Consensus sequences are highlighted.

sequenced, two clear consensus sequences, highlighted in Figure 8, were observed. The consensus sequences fall into two groups, which show substantial homology. In addition, some of the sequences were found to be present in many different clones. This shows that there are only a few solutions to generating high-affinity binding RNA molecules directed towards tobramycin. Furthermore, this result is also consistent with expectations based on the amplification factors observed in the two selections. After starting with 10^{15} RNA molecules and selecting $1:10^7$ in two rounds of amplification, one would expect that there should be only 10 high-affinity sequences in the starting material.

The binding of tobramycin to two cloned RNAs (X1 and J6, Fig. 8), representing each class of consensus sequences, was measured using the fluorescence techniques already described (Table 2). As expected, the binding of tobramycin to both RNAs (X1 and J6) was of high affinity. However, in these cases two molecules of tobramycin are bound to each RNA molecule; one tobramycin molecule binds specifically in a high-affinity mode and the other binds specifically in a low-affinity mode. A saturation binding curve showing the biphasic binding behavior of J6 RNA is shown in Figure 9. The high-affinity component binds tobramycin 10^3 times more tightly than do sensitive ribosomes [15].

The consensus sequences determined for the two groups of high-affinity binding RNAs probably form part of the tobramycin-binding region. Accordingly, we would expect that these sequences would be found in non-base-paired regions of the RNA. RNA secondary structure analysis of the two RNA molecules, using the program MFOLD [19], indicates that this indeed may be the case. Two representative lowest energy structures are shown in Figure 10, illustrating that the consensus sequences exist in stem–loop structures. The predicted stem–loop structures of both X1 and J6 were prepared with extra G–C base pairs to secure the stem–loop structure. As expected, analysis of these minimal RNAs by MFOLD generated the structures shown in Figure 10. Both minimal stem–loop structures bound tobramycin with high affinity (Table 2) and with the same 2:1 stoichiometry that was observed with X1 and J6. Thus, the tobramycin binding sites of X1 and J6 are probably located in the stem–loops. It should be noted that, in the case of the X1 stem–loop, the shorter chain analog of PYT (6'-N-4-pyreneacetyl tobramycin), was required to give quantitatively useful fluorescence quenching.

Discussion

One approach to exploring the rules that govern RNA–antibiotic interactions is first to determine if particular RNA molecules can be selected that bind specifically to certain antibiotics, then determine the structures of these complexes. We have selected RNA molecules that can bind to the aminoglycoside tobramycin with high affinity. Although less than 0.1 % of the total RNA applied to the initial tobramycin affinity column was specifically eluted with tobramycin, the specific binding pool could be increased to 82 % after six cycles of selections. It can be calculated that the experiments began with at most ~10^{15} sequences. The six cycles of selection amplified the tobramycin-binding aptamers by a factor of ~10^7, leaving a maximum of ~10^8 sequences that can bind tobramycin with a K_d in the 10μM range. In practice, it would be expected that the functional diversity of this pool is probably reduced by a factor of ~10 due to

Table 2. Dissociation constants of RNA aptamers.

	J6	X1	J6sl	X1sl
K_1(PYT) (nM)	5.4±0.5[a]	7.6±1.1[a]	286±10[a]	65.1±7.4[b]
K_1(TOB) (nM)	2±1	3±1	9±3	12±5
K_2(TOB) (μM)	6.0±0.4	15.9±0.7	2.7±0.3	13.2±0.5

Binding measurements were made at 20 °C as described in Materials and methods. The high affinity component for [a]PYT, or [b]6'-N-4-pyreneacetyl tobramycin, is measured along with both high- and low-affinity components (K_1 and K_2, respectively) for the binding of tobramycin (TOB). Values for binding to J6, X1 and their stem–loop (sl) counterparts are given.

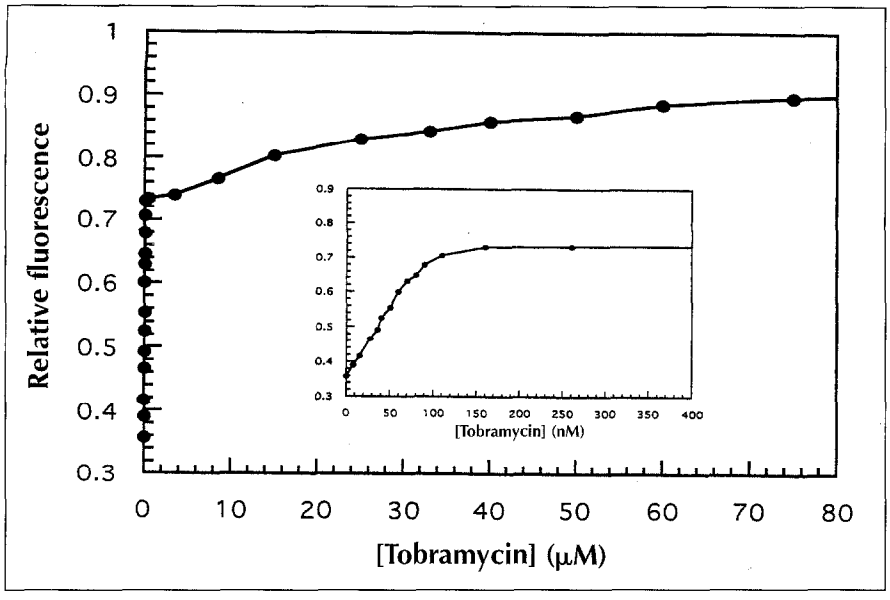

Fig. 9. Fluorescence titration of PYT solution containing J6-RNA as a function of tobramycin concentration. [PYT] = 15.0 nM, [J6-RNA] = 35nM. Tobramycin binds to J6-RNA in high and low affinity modes. The insert shows the high affinity binding in an expanded scale.

limitations in the chemistry of oligomer synthesis. So it is likely that there are in the neighborhood of 10^7–10^8 RNA sequences in the selected pool that can bind tobramycin. This is interesting because it suggests that there are many different ways for an RNA molecule to recognize an aminoglycoside with a moderately high affinity.

The DNA from reverse-transcription of the random aptamer pool was cloned in order to analyze individual sequences. Plasmid DNA from 18 clones was sequenced. No two of the sequences were identical, and no consensus sequence was observed. The great diversity of the pool is reflected in the observation that the 18 sequences cloned were all unique. It is clear that RNA structures can be organized in many different ways to recognize tobramycin with μM affinity. Of course it is possible that many of these RNA structures are similar in local structure. Since tobramycin is polycationic at the pH studied, electrostatic interactions between the

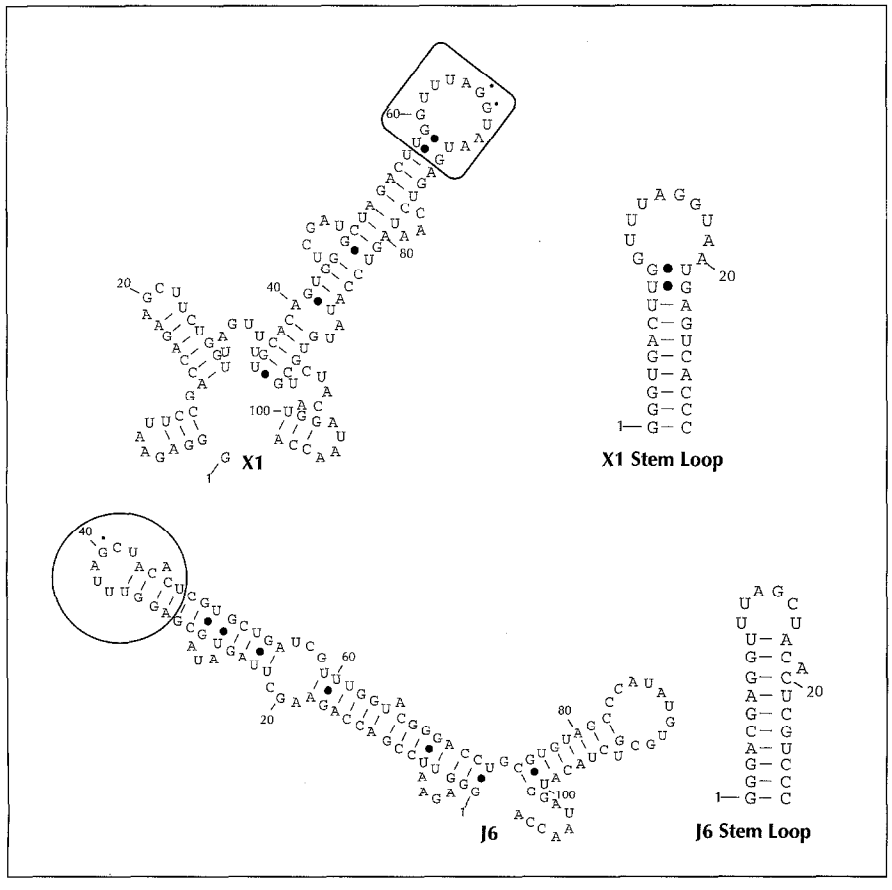

Fig. 10. Minimized structures for X1, J6 and corresponding stem–loops. Outlined areas indicate consensus regions. The stem–loops are constructed with extra G–C base pairs to secure the structures. The bold dots indicate wobble base pairs and the small dots in the outlined areas indicate non-consensus bases.

drug and RNA, along with hydrogen bonding, are probably important in mediating recognition. This being the case, base-sequence specificity *per se* would not be expected to be of overriding importance, because tobramycin is unlikely to be recognizing specific sequences of nucleotides.

The RNA from this combined pool exhibited an average K_d for tobramycin of ~8.8 μM. This is an interesting result, because this is close to the K_d measured for the specific binding of tobramycin to sensitive ribosomes [15]. From the studies reported here, there are clearly many RNA sequences that bind to tobramycin with K_d values in the μM range. Why there might be such a limited number of specific tobramycin binding sites in ribosomes is understandable in terms of the possible RNA diversity in cells. It must be remembered that, in the work reported here, only one RNA sequence in ~10^7 sequences can bind tobramycin.

Although it is clearly impractical to study the specificity of binding of all of the clones quantitatively, we did study one clone (W13) in some detail. Equilibrium dialysis showed that the K_d of W13 for acetyl tobramycin was 1.3 μM and that for tobramycin was 3.0 μM. These values are close to the K_ds of these compounds measured for ribosomes. The measured K_d for the binding of acetyl tobramycin to *E. coli* ribosomes is 3.3 μM, and that for tobramycin itself is 1.1 μM [15].

To better assess the specificity of tobramycin binding to W13 RNA, a fluorescence protocol using PYT was developed. The fluorescence emission intensity of this probe was strongly quenched upon binding to the RNA. This quenching led to ready measurements of the stoichiometry and specificity of binding. The measured K_d for binding of PYT to W13 is 20 nM, a value which represents a ~200-fold increase in affinity over that found with tobramycin. The enhanced binding is doubtless a function of the pyrene moiety, because simply acetylating the primary amino group of tobramycin does not lead to significantly enhanced binding to the RNA. It will be interesting to determine if the binding affinity of aminoglycosides in general can be enhanced by this kind of modification. The stoichiometry of binding of PYT to clone W13 RNA proved to be 1:1, suggesting a specific mode of interaction.

The fluorescence assay made it possible to measure the competition of various ligands for the aminoglycoside binding site directly. Tobramycin itself competed for binding to the aminoglycoside binding site, and its K_d was measured to be 4.3 μM, a value close to that measured by the equilibrium dialysis technique. Glucosamine did not measurably compete with PYT binding, showing that simple non-specific binding to charged amino sugars is not the basis for the observed binding. Erythromycin (Fig. 11), an antibiotic structurally dissimilar from tobramycin, only weakly inhibited PYT binding. By contrast, the two aminoglycosides, gentamycin C and in particular neomycin B, proved to be reasonably potent inhibitors of binding (Fig. 11). Interestingly, both gentamycin and neomycin inhibit the splicing of group I introns about as efficiently as does tobramycin itself [3]. In addition, both of these drugs also blocked the binding of acetyl tobramycin to *E. coli* ribosomes [15]. Thus it appears that similar structural features in RNA are recognized by tobramycin, gentamycin and neomycin.

The studies reported here show that there are many low-affinity (~μM) solutions to the binding of the aminoglycoside tobramycin by RNA aptamers. From the selected population of low-affinity aptamers we

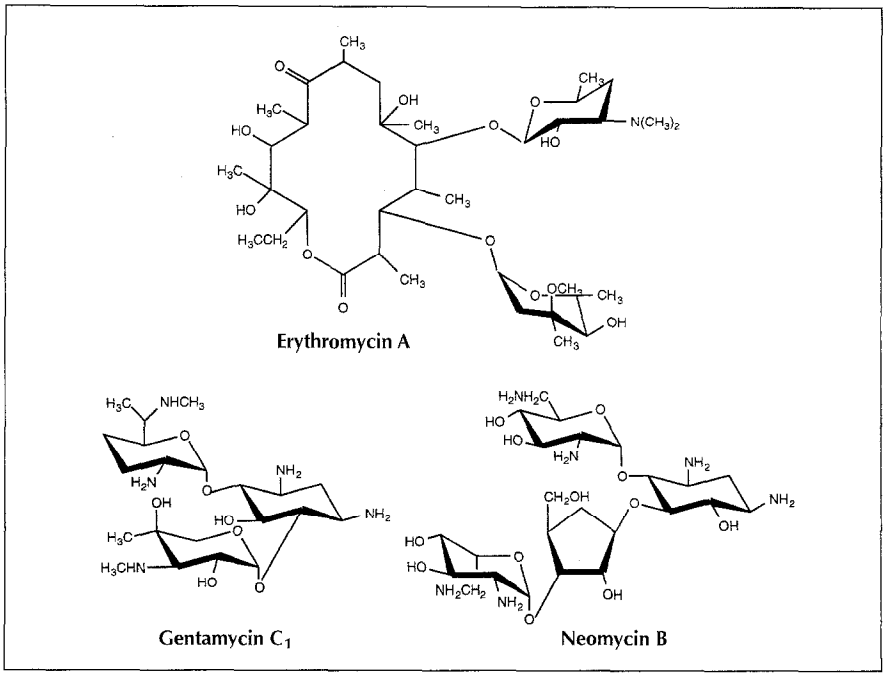

Fig. 11. Antibiotics studied as competitive-binding inhibitors.

were able to isolate relatively few high-affinity (~nM) solutions. However, it is possible that many of the high-affinity aptamers were lost during the early rounds of selection when the copy number is low because they could not be eluted from the affinity column during the washes with 10 mM tobramycin. Molecules with high affinity to the column might have a very slow off rate and thus be less likely to bind to free tobramycin and be recovered in the eluant. For this reason, it is difficult to estimate the frequency of tight-binding aptamers in the initial pool with certainty.

Approximately 10^7–10^8 sequences capable of binding tobramycin with moderate affinity were found after the first selection. A further 10^7 enrichment occurred during the higher stringency selection. It is not surprising, then, that few solutions exist for high-affinity tobramycin binding after the high-stringency selection. Two different consensus sequences were observed, as exemplified by X1 and J6. Secondary-structure analysis using MFOLD suggested that the consensus sequences in these two constructs were located in stem–loop regions. Although two different consensus sequences were observed, they do show homology. In fact, the X1 and J6 stem–loop structures could de drawn to give nearly identical loops (UUAGNU). The hypothesis that these putative loop structures contain the binding regions of the aminoglycosides will be tested by mutational studies and by chemical footprinting.

The analysis discussed above suggests the working hypothesis that the binding of aminoglycoside occurs in a simple stem–loop or in a stem–loop with a bulge, and thus higher order RNA structures may be important in specific binding phenomena. Evidence for this notion comes from the independent preparation of the predicted stem–loop and stem–loop with a bulge regions, and the demonstration that these constructs bound tobramycin with nearly the same affinities as did the selected aptamers. Moreover, these stem–loop structures also bound two molecules of tobramycin, just like their aptamer precursors X1 and J6. It is interesting to note that the lower affinity aptamer W13 only bound one molecule of aminoglycoside. Whether there is a relationship between the affinity of aptamer binding to tobramycin and the stoichiometry of drug binding is currently unknown. Another difference between the lower and higher affinity binders is found in the enhanced binding, relative to tobramycin, of the fluorescent derivative PYT to the lower affinity aptamer W13. It is possible that the higher affinity sites are more structured than their low-affinity counterparts, and hence less susceptible to interacting with the pyrene moiety of PYT.

Structural studies on the putative stem–loop constructs will determine the molecular basis for tobramycin recognition. Moreover, a direct structural comparison of the high- and low-affinity binding aptamers should provide important information on how to design high-affinity RNA-binding ligands. It will also be of interest to understand how two molecules of tobramycin are bound to the X1 and J6 stem–loops, and whether a conformational change in the RNA accompanies the binding of the first molecule of aminoglycoside, enabling the second molecule to bind.

Significance

In this study, we found that specific RNA aptamers that bind the aminoglycoside antibiotic tobramycin can readily be selected from a randomized pool. The average K_d for the pool selected under low stringency is in the μM range. The RNA synthesized from an individual clone chosen at random bound tobramycin with a 1:1 stoichiometry and with about the same affinity as observed for the binding of tobramycin to ribosomes and introns. Selection at greater stringency led to the discovery of the highest affinity binding recorded for the binding of any small molecule to an RNA or DNA aptamer. Here clear consensus sequences, located in predicted stem–loop structures, were found. Minimal sequences predicted to form these stem–loop structures were synthesized and were capable of binding tobramycin with high affinity.

The approaches reported here should be generally applicable to the study of the binding of other aminoglycoside antibiotics and small molecules to RNA. In particular, fluorescently labeled antibiotics should be useful for analyzing the interactions of aminoglycosides with RNA. When coupled with the use of high-resolution NMR and X-ray spectroscopic studies, it ought to be possible to define the specific ways in which RNA molecules recognize aminoglycoside antibiotics. This information will be important in the design of novel molecules that will bind to and interfere with the function of specific RNA structures. Molecules of this type could be useful as paradigms for the design of novel drugs.

Materials and methods

Reagents

Affi-Gel 10 was purchased from Bio Rad. Tobramycin, neomycin trisulfate trihydrate (neomycin B > 90 %), ethanolamine, erythromycin, gentamycin sulfate (gentamycin C > 99 %), N-hydroxysuccinimide, N,N-dicyclohexylcarbodiimide, 1-pyrenebutyric acid, D-glucosamine and N,N-dimethylformamide were from Fluka. Amberlit CG-50, tetracycline and ampicillin were from Sigma. ^{3}H-acetic anhydride was from American Radiolabeled Chemicals. α-^{32}P-rATP and α-^{35}S-dATP were from New England Nuclear. Sephadex G-50 was from Pharmacia. The GeneAmp PCR kit, GeneAmp Thermostable rTth Reverse Transcriptase RNA PCR kit and Amplicycle Sequencing kit were from Perkin Elmer. The two primers used and the 109-mer random DNA pool were purchased from Oligos Etc., Inc. Restriction enzymes *Eco*RI and *Bam*HI were from Boehringer Mannheim. pBluescript II SK(–) phagemid, XL1-Blue MRF', *E. coli* host

cells and the KS primer were from Stratagene. The Wizard Miniprep DNA Purification System was from Promega.

Synthesis of 6-N-^{3}H-acetyl tobramycin

Radiolabeled acetyl tobramycin was prepared by the published procedure [15], but was purified by ion exchange chromatography (see synthesis of PYT for details of ion exchange methods) rather than by preparative thin layer chromatography. The R_f = 0.62 on silica (NH_4OH:methanol:n-butanol = 5:4:3). MS(FAB) = 510/$(M+H)^+$.

Synthesis of 6'-N-4-pyrenebutyryl tobramycin (PYT)

1-Pyrenebutyric acid (1.0 g; 3.5 mmol) and N-hydroxysuccinimide (0.40 g; 3.5 mmol) were dissolved in 40 ml dioxane. To this solution was added N,N-dicyclohexylcarbodiimide (0.72 g; 3.5 mmol). After reaction at room temperature for 4 h, the N-hydroxysuccinimide ester of 1-pyrenebutyric acid (PYS) product was purified by repeated recrystallization from isopropanol. Final yield = 0.87 g (65 %). TLC (silica):R_f = 0.56 ($CHCl_3$:MeOH = 20:1). MS (EI): 385/M^+.

Tobramycin (100 mg; 0.21 mmol) and PYS (81 mg; 0.21 mmol) were dissolved in 1.5 ml dimethylformamide (a small amount of H_2O was added to fully dissolve tobramycin). After reacting at room temperature for 1 h, the reaction mixture was diluted with 20 ml H_2O, filtered, and applied to an Amberlit CG-50 column (5 x 120 mm). The column was washed with 50 ml H_2O, 50 ml 0.1 M NH_4OH and finally 0.25 M NH_3OH; the final elution gave the pure PYT, 40 mg (yield = 26 %). TLC (silica):R_f = 0.62 (H_2O: methanol: n-butanol:NH_4OH = 5:4:3:1). MS (FAB): 738/$(M+H)^+$. The synthesis of 6'-N-4-pyreneacetyl tobramycin was carried out in an identical way to the synthesis of PYT except for the substitution of 1-pyreneacetic acid for 1-pyrenebutyric acid.

Affinity column preparation

An N-hydroxysuccinimide Affi-Gel column was derivatized with either 20 μmoles or 0.075 μmoles tobramycin per ml of gel to generate the affinity columns. Excess N-hydroxysuccinimide linkages were blocked by adding 1 M ethanolamine. The resulting column served as the support for the RNA selections. According to data provided by the manufacturer, the number of reactive sites on the column was estimated as about 15 mM. Selections were performed in 1 ml column volumes in a buffer (selection buffer) containing 140 mM NaCl, 5 mM KCl, 1 mM $CaCl_2$, 1 mM $MgCl_2$ and 20 mM Tris acetate at pH 7.4 [20]. A 1 ml Affi-Gel 10 pre-column treated with ethanolamine was used in all selections.

Preparation of nucleic acid pools and selections

The original double-stranded DNA pool was constructed by large scale PCR amplification of the synthesized 109-mer containing 60 random nucleotides. Sixty μg of the synthesized 60-mer (109 nucleotides including primers that were identical to those previously described [16]) containing a maximum of ~10^{15} individual sequences was used for a 10-ml scale PCR reaction. The original RNA pool was constructed by reverse-transcription of 120 μg double stranded DNA. ^{32}P-labeled RNA was used to follow all selections. RNA, purified by Sephadex G-50 column chromatography to remove unincorporated nucleotides, was heated at 75 °C for 5 min, and then cooled down to room temperature. The RNA was then applied to the pre-column and washed directly onto the tobramycin affinity column with 1 ml of buffer. This was followed by washing with 20 column volumes of the buffer. Specifically bound RNAs were eluted with three column volumes of 10 mM tobramycin in the selection buffer. For the first round, 1.3 mg of RNA was used; in succeeding rounds 40–60 μg of RNA was used. The RNA was precipitated with ethanol, with glycogen as a carrier. RNA reverse transcription and PCR were performed in a single tube, using a GeneAmp Thermostable rTth Reverse Transcriptase RNA PCR kit (Perkin Elmer). About 50 ng of RNA template was used for 20 μl scale reverse-transcription reactions. The succeeding PCR reaction was done for only 4–8 thermocycles to ensure high quality of the PCR products. Cloning of PCR DNA products was conducted using a pBluescript II SK(–) phagemid cloning vector and an XL1-Blue MRF' *E. coli* as the host bacteria.

Fluorescence measurements

Steady-state fluorescence measurements were performed on a Perkin Elmer Model 512 double beam fluorescence spectrometer. The excitation wavelength was 341 nm. All measurements were done at 20 °C in 140 mM NaCl, 5 mM KCl, 1 mM $CaCl_2$, 1 mM $MgCl_2$ and 20 mM HEPES (pH=7.4). The K_d of the PYT and the RNA aptamer was calculated by curve fitting of the fluorescence intensity as a function of [RNA], using the following equation (assuming a 1:1 complex):

$$I = I_0 + 0.5\Delta\epsilon([PYT]_0 - (([PYT]_0 + [RNA]_0 K_I)^2 - 4[PYT]_0[RNA]_0)^{0.5}) \quad \textbf{(Equation 1)}$$

where I_0 and I are the fluorescence intensities of PYT in the absence and presence of RNA, respectively, and $\Delta\epsilon$ is the difference between the fluorescence intensities of 1 μM PYT in the presence of an infinite concentration of RNA and in its absence. $[RNA]_0$ is the total concentration of RNA added; $[PYT]_0$ is the total concentration of PYT.

Competition binding measurements of antibiotics with RNA and PYT were performed at constant concentrations of PYT and RNA by monitoring fluorescence intensity changes as a function of changing concentrations of the antibiotics. The K_ds for the antibiotics were calculated by curve fitting of the fluorescence intensity of PYT as a function of antibiotic concentration, using the following equation:

$$I = I_0 + \Delta\epsilon[PYT \bullet RNA] \quad \textbf{(Equation 2)}$$

where $[PYT \bullet RNA] = 0.5((([PYT]_0 + [RNA]_0)([RNA]_0 + K_d) + K_I([T]_0 + [RNA]_0 + K_d) - ((([PYT]_0 + [RNA]_0)([RNA]_0 + K_d) + K_I([T]_0 + [RNA]_0 + K_d))^2 - 4([RNA]_0 + K_d)[PYT]_0[RNA]_0([RNA]_0 + K_d))^{0.5}/([RNA]_0 + K_d)$. K_d and K_I are the dissociation constants for the antibiotic and PYT, respectively. $[T]_0$ is the total concentration of antibiotic added. Measurements were taken at least twice for each measured K_d.

Equilibrium dialysis

Equilibrium dialysis measurements were performed by the published procedure [21].

Acknowledgements: We gratefully acknowledge the technical assistance of Ms G. Chang. This work was supported by the Ruth and Milton Steinbach Fund, Inc. and the National Institutes of Health U.S. Public Health Service Grants EY03624 and EY04096.

References

1. Cundliffe, E. (1989). How antibiotic-producing organisms avoid suicide. *Annu. Rev. Microbiol.* **43**, 207–233.
2. Cundliffe, E. (1990). Recognition sites for antibiotics within rRNA. In *The Ribosome: Structure, Function & Evolution.* (Hill, W.E., Dahlberg, A.E., Garrett, R.A., Moore, P.B., Schlessinger, D. & Warner, J.R., eds), pp. 479–490, American Society for Microbiology, Washington, DC.
3. von Ahsen, U., Davies, J & Schroeder, R. (1991). Antibiotic inhibition of group I ribozyme function. *Nature* **353**, 368–370.
4. von Ahsen, U. & Noller, H.F. (1993). Footprinting the sites of interaction of antibiotics with catalytic group I intron RNA. *Science* **260**, 1500–1503.
5. Woodcock, J., Moazed, D., Cannon, M., Davies, J. & Noller, H.F. (1991). Interaction of antibiotics with A- and P-site-specific bases in 16S ribosomal RNA. *EMBO J.* **10**, 3099–3103.
6. Hutchin, T., *et al.*, & Cortopassi, G. (1993). A molecular basis for human hypersensitivity to aminoglycoside antibiotics. *Nucleic Acids Res.* **21**, 4174–4179.
7. Purohit, P. & Stern, S. (1994). Interactions of a small RNA with antibiotic and RNA ligands of the 30S subunit. *Nature* **370**, 659–662.
8. Schroeder, R., Streicher, B. & Wank, H. (1993). Splice-site selection and decoding: are they related? *Science* **260**, 1443–1444.
9. Stage, T.K., Hertel, K.J. & Uhlenbeck, O.C. (1995). Inhibition of the hammerhead ribozyme by neomycin. *RNA* **1**, 95–101.
10. Zapp, M.L., Stern, S. & Green, M.R. (1993). Small molecules that selectively block RNA binding of HIV-1 Rev protein inhibit Rev function and viral production. *Cell* **74**, 969–978.
11. Ellington, A.D. & Szostak, J.W. (1990). *In vitro* selection of RNA molecules that bind specific ligands. *Nature* **346**, 818–822.
12. Tuerk, C. & Gold, L. (1990). Systematic evolution of ligands by exponential enrichment. *Science* **249**, 505–510.
13. Beaudry, A. & Joyce, G. F. (1992). Directed evolution of an RNA enzyme. *Science* **257**, 635–641.
14. Tangy, F., Capmau, M.-L. & LeGoffic, F. (1983). Photo-induced labelling of *E. coli* ribosomes by a tobramycin analog. *Eur. J. Biochem.* **131**, 581–587.
15. LeGoffic, F., Capmau, M.-L., Tangy, F. & Baillarge, M. (1979). Mechanism of action of aminoglycoside antibiotics. *Eur. J. Biochem.* **102**, 73–81.
16. Famulok, M. & Szostak, J.W. (1992). Stereospecific recognition of tryptophan agarose by an *in vitro* selected RNA. *J. Am. Chem. Soc.* **114**, 3990–3991.
17. Kierzek, R., Li, Y., Turner, D.H. & Bevilacqua, P.C. (1993). 5'-Amino pyrene provides a sensitive, nonperturbing fluorescent probe of RNA secondary and tertiary structure formation. *J. Am. Chem. Soc.* **115**, 4985–4992.
18. Bevilacqua, P.C., Li, Y. & Turner, D.H. (1994). Fluorescence-detected stopped flow with a pyrene labeled substrate reveals that guanosine facilitates docking of the 5' cleavage site into a high free energy binding mode in the *Tetrahymena* ribozyme. *Biochemistry* **33**, 11340–11348.
19. Jaeger, J.A, Turner, D.H. & Zuker, M. (1989). Predicting optimal and suboptimal secondary structure for RNA. *Methods Enzymol.* **183**, 281–306.
20. Bock, L.C., Griffin, L.C, Latham, J.A, Vermaas, E.H. & Toole, J.J. (1992). Selection of single-stranded DNA molecules that bind and inhibit human thrombin. *Nature* **355**, 564–566.
21. Lorsch, J.R. & Szostak, J.W. (1994). *In vitro* selection of RNA aptamers specific for cyanocobalamin. *Biochemistry* **33**, 973–982.

Received: **24 Mar 1995**; revisions requested: **4 Apr 1995**; revisions received: **19 Apr 1995**. Accepted: **19 Apr 1995**.